

# Origins of Selective C(sp<sup>2</sup>)-H Activation Using Transition Metal Complexes with N,N-Bidentate Directing Groups: A Combined Theoretical-Experimental Study

Hao Tang,<sup>†,§</sup> Bingwei Zhou,<sup>‡</sup> Xu-Ri Huang,<sup>\*,§</sup> Congyang Wang,<sup>\*,‡</sup> Jiannian Yao,<sup>†</sup> and Hui Chen<sup>\*,†</sup>

<sup>†</sup>Beijing National Laboratory for Molecular Sciences (BNLMS), CAS Key Laboratory of Photochemistry, Institute of Chemistry, Chinese Academy of Sciences, Beijing 100190, People's Republic of China

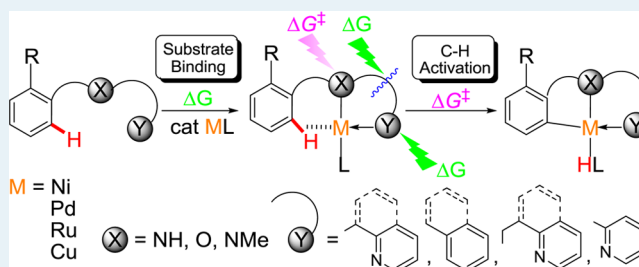
<sup>‡</sup>Beijing National Laboratory for Molecular Sciences (BNLMS), CAS Key Laboratory of Molecular Recognition and Function, Institute of Chemistry, Chinese Academy of Sciences, Beijing 100190, People's Republic of China

<sup>§</sup>Institute of Theoretical Chemistry, State Key Laboratory of Theoretical and Computational Chemistry, Jilin University, Changchun, 130023, People's Republic of China

## S Supporting Information

**ABSTRACT:** The strategy using N,N-bidentate directing groups is a promising way to achieve selective C(sp<sup>2</sup>)-H activation inaccessible by that of monodentate directing groups. Herein, through theoretical calculations, we present a rationale behind this strategy, which deciphers its key roles in C-H activation promoted by Ni, Pd, Ru, and Cu. The calculations reveal two key points: (a) Between the two coordination sites of the N,N-bidentate directing group, the proximal one influences more the C-H activation barrier  $\Delta G^\ddagger$ , whereas the distal site affects more the free energy change  $\Delta G$  relevant to the substrate coordination. (b) Enlarging/shrinking the chelation ring can exert different effects on the reactivity, depending on the metal identity and the ring size. Importantly, our computational results are in full agreement with previous experimental findings concerning reactivity. Furthermore, a prediction about the unprecedented reactivity from our theory is confirmed by our experiments, lending more credence to the rationale and insights gained in this study.

**KEYWORDS:** N,N-bidentate directing group, C(sp<sup>2</sup>)-H activation, transition metal, coordination free energy, reaction barrier, density functional theory



## 1. INTRODUCTION

The transition-metal-catalyzed C-H activation reaction has emerged as one of the most promising and powerful methods for the direct conversion of inert C-H bonds into C-C and C-X (X = heteroatom) bonds in recent years.<sup>1</sup> Chelation assistance is currently in widespread use in such transformations of C-H bonds because it enables the efficient and selective cleavage of the proximal C-H bond through a cyclometalation reaction.<sup>2</sup> A wide variety of directing groups have been reported, and in most cases, monodentate directing groups were utilized, the role of which in C-H activation has been extensively explored both experimentally and computationally (Scheme 1a).<sup>2,3</sup> Recently, bidentate-type directing groups have provided new possibilities for exploring challenging C-H transformations that could not be achieved by adopting monodentate directing groups (Scheme 1b).<sup>4</sup>

Since the pioneering study of Daugulis et al.,<sup>5</sup> who reported the arylation of unactivated C-H bonds using 8-aminoquinoline and picolinamides as N,N-bidentate directing groups in conjunction with Pd(OAc)<sub>2</sub> as a catalyst, a number of reactions utilizing N,N-bidentate directing groups have been developed for Pd(II)-catalyzed reactions.<sup>6,7</sup> On the basis of this strategy,

ortho C(sp<sup>2</sup>)-H bond activation/transformation has also been successfully realized in Ni-,<sup>8</sup> Ru-,<sup>9</sup> and Cu-catalyzed/-promoted<sup>10</sup> reactions. As excellent examples, Chatani et al. reported Ni(0)-catalyzed oxidative annulation of aromatic amides with alkynes, resulting in the formation of isoquinolones<sup>8a</sup> as well as Ni(II)-catalyzed alkylation of C-H bonds with unactivated alkyl halides.<sup>8b</sup> Later, this strategy was also successfully applied in Ru(II)-catalyzed arylation of C-H bonds in aromatic amides.<sup>9c</sup> Quite recently, Miura et al. reported copper-mediated C-H/C-H coupling of benzoic acid derivatives and 1,3-azoles with the aid of the 8-quinolinylamine-based double N,N-coordination strategy.<sup>10b</sup>

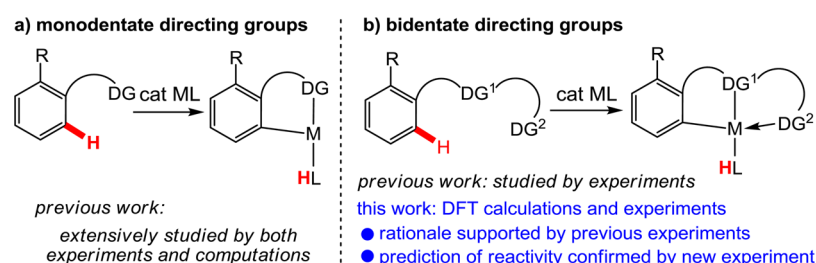
Although C-H bond activation utilizing bidentate chelation is well established experimentally, a predictive theoretical understanding of the effectiveness of this strategy is still missing. Specifically, quantitative assessment of the roles of bidentate chelation in a complex catalytic reaction, particularly in the key step of C-H bond activation, is not yet known.

Received: December 3, 2013

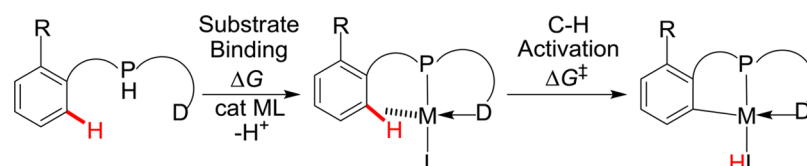
Revised: January 11, 2014

Published: January 13, 2014

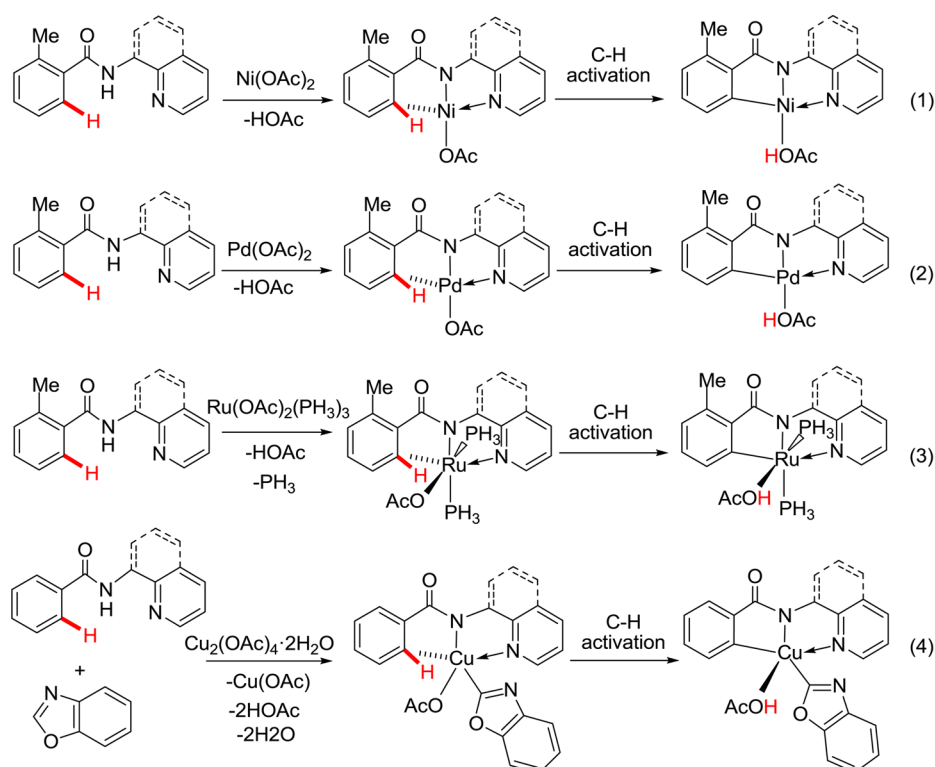
Scheme 1. The N,N-Bidentate Directing Group Strategy for C–H Activation



Scheme 2. The Reaction Model for C–H Activation Utilizing Bidentate Chelation Strategy



Scheme 3. C–H Activation Studied in This Work



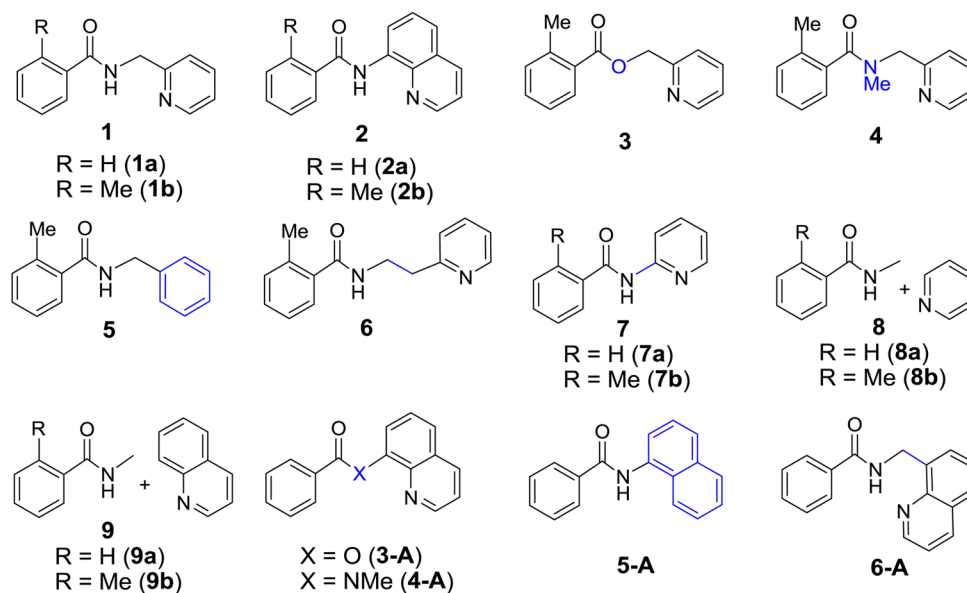
Although previous theoretical studies on monodentate directing groups<sup>3,11</sup> have contributed considerable insights into the C–H activation chemistry, theoretical efforts toward understanding bidentate directing groups are rarely seen, with only sporadic attempts on a few isolated reactions or selectivity.<sup>12</sup> With density functional theory (DFT) computations, this work presents a theory for rationalizing N,N-bidentate chelation in C–H activation, which is consistent with previous experimental findings, and we also confirm its prediction by our own reactivity experiments.

## 2. METHODS

All calculations were performed using the Gaussian 09 suite of programs.<sup>13</sup> For geometry optimization in the gas phase, the hybrid B3LYP density functional<sup>14</sup> was used in combination

with the def2-SVP basis set<sup>15</sup> (B1) for all the atoms. All of the geometries were fully optimized without symmetry constraints. Vibrational analysis calculations were performed to verify the nature of the stationary points and also to obtain the thermal free energy correction. All optimized transition states (TSs) described in this work have only one proper imaginary frequency, whereas minima have no imaginary frequencies. All the C–H activation TSs were verified to lead to the corresponding cyclometalated intermediates through IRC calculations. To refine the electronic energy, single point calculations with larger basis sets were carried out on these optimized structures with the B3LYP functional using the def2-TZVP basis set<sup>15</sup> (B2) for all elements. To take the solvent effect into account, the continuum solvation model SMD<sup>16</sup> was utilized in all the single point calculations using the B2 basis set.

Scheme 4. Substrates Explored in This Work



The experimentally employed solvents (toluene for reactions 1–3 and *o*-xylene for reaction 4) were used in solvent effect modeling as the solvents. The reported energies in this work include the B2 electronic energy in solution, DFT-D3 empirical dispersion correction proposed by Grimme et al.,<sup>17</sup> gas phase thermal correction to the Gibbs free energy, and solvation free energy. The thermal correction to the Gibbs free energy was calculated at the corresponding experimental reaction temperature of 140, 110, 140, and 135 °C for reactions 1, 2, 3, and 4, respectively. Experimental details can be found in the Supporting Information (SI) document.

### 3. RESULTS AND DISCUSSION

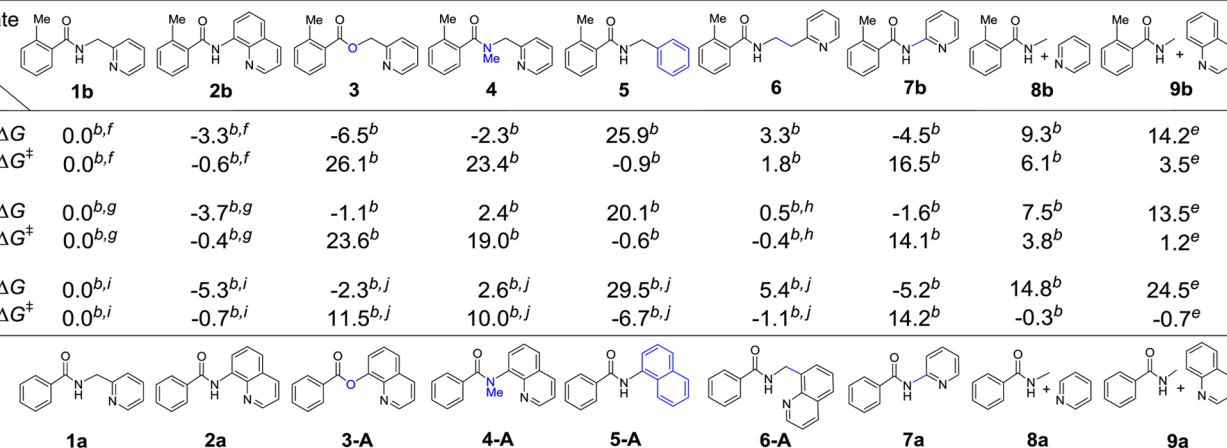
Our basic model for C–H activation is consistent with the current consensus on the reaction scheme of C–H activations assisted by directing groups.<sup>2,3</sup> As shown in Scheme 2, the substrate first coordinates to a metal center to form a C–H preactivated intermediate, associated with a Gibbs free energy change,  $\Delta G$ , that measures the tendency of this intermediate formation for substrate binding. After this C–H preactivated intermediate is generated, the C–H bond could be cleaved, the ease of which is characterized by a C–H activation free energy barrier  $\Delta G^\ddagger$ . Of note, this C–H activation model is quite similar to the Michaelis–Menten model of classic enzymatic catalysis.<sup>18</sup> According to transition state theory and thermodynamic equilibrium of the reactant complexation before C–H activation, both  $\Delta G$  and  $\Delta G^\ddagger$  should collectively control the reaction rate of the C–H cleavage step in C–H activation. As shown in this work, by computing and comparing these two key parameters ( $\Delta G$  and  $\Delta G^\ddagger$ ) of the above reaction model, we are able to decipher the origin of the reactivity in C–H activation enabled by the N,N-bidentate chelation strategy.

On the basis of the elegant experimental reports utilizing N,N-bidentate chelation strategy,<sup>7c,8b,9c,10b</sup> as depicted in Scheme 3, in this work, we studied the corresponding C–H activation reactions (1–4) mediated/catalyzed by four transition metals (Ni, Pd, Ru, and Cu). These selected cases include a rich coordination environment for central transition metals. Among them, d<sup>8</sup> Ni(II) and Pd(II) complexes adopt the typical four-coordinate square-planar geometry, and d<sup>8</sup> Cu(III)

species possess either four-coordinate square-planar geometry or an additional weak axial coordination leading to five-coordinate tetragonal pyramid geometry. For the d<sup>6</sup> Ru(II) case, as usual, a six-coordinate octahedral structure is involved. The above wide ranges of the coordination environment provide an opportunity for us to explore both the system-dependent and system-independent roles played by a bidentate directing group in C–H activation reactivity, the latter of which would shed more light on the general understanding of the bidentate directing group.

To explore and reveal the origin of the effectiveness of N,N-bidentate directing groups, we considered plenty of substrates in our computational modeling, as shown in Scheme 4. In previous experiments,<sup>7c,8,9a,c,d,10b</sup> many of these substrates have been examined; thus, they can herein serve as representative examples to test our theory on reactivity. The key idea in our theoretical description of C–H activation reactivity is the comparison between different substrates to get  $\Delta\Delta G$  and  $\Delta\Delta G^\ddagger$  from their  $\Delta G$  and  $\Delta G^\ddagger$ . Of note is that  $\Delta G$  contains free energy changes caused not only by the substrate binding, but also from other processes necessary to generate the C–H preactivated intermediate from the source metal complexes, such as the disproportionation of Cu(II) to generate reactive Cu(III), shown in reaction 4 (see Scheme 3). Despite this mixing of information in  $\Delta G$ , by comparison of the different substrates within one specific reaction system, we are able to remove these “noises” irrelevant to the substrate binding because they are canceled in subtraction of two  $\Delta G$ 's to get  $\Delta\Delta G$ . Since the difference in the  $\Delta G$  values to be compared lies only in substrates,  $\Delta\Delta G$  obtained thereby can faithfully exhibit the binding energy difference between different substrates. In this comparative way,  $\Delta\Delta G$  and  $\Delta\Delta G^\ddagger$  convey confined information of relative energetics for substrate binding and C–H activation, respectively. Consequently, for each reaction, we need to choose substrates as reference, and in practice, we usually select experimentally reactive ones. By comparing with the reference substrate that is known to be reactive in experiment, the relative reactivity of a specific substrate can be estimated. Such a way of describing the reactivity in a relative manner can also more tolerate the

Table 1. Calculated Relative Reaction Binding Free Energies ( $\Delta\Delta G$ ) and Barriers ( $\Delta\Delta G^\ddagger$ ) in kcal/mol<sup>a</sup>

reaction/ catalyst	substrate																		
		1b	2b	3	4	5	6	7b	8b	9b	1a	2a	3-A	4-A	5-A	6-A	7a	8a	9a
1/Ni(II)	$\Delta\Delta G$	0.0 <sup>b,f</sup>	-3.3 <sup>b,f</sup>	-6.5 <sup>b</sup>	-2.3 <sup>b</sup>	25.9 <sup>b</sup>	3.3 <sup>b</sup>	-4.5 <sup>b</sup>	9.3 <sup>b</sup>	14.2 <sup>e</sup>									
	$\Delta\Delta G^\ddagger$	0.0 <sup>b,f</sup>	-0.6 <sup>b,f</sup>	26.1 <sup>b</sup>	23.4 <sup>b</sup>	-0.9 <sup>b</sup>	1.8 <sup>b</sup>	16.5 <sup>b</sup>	6.1 <sup>b</sup>	3.5 <sup>e</sup>									
2/Pd(II)	$\Delta\Delta G$	0.0 <sup>b,g</sup>	-3.7 <sup>b,g</sup>	-1.1 <sup>b</sup>	2.4 <sup>b</sup>	20.1 <sup>b</sup>	0.5 <sup>b,h</sup>	-1.6 <sup>b</sup>	7.5 <sup>b</sup>	13.5 <sup>e</sup>									
	$\Delta\Delta G^\ddagger$	0.0 <sup>b,g</sup>	-0.4 <sup>b,g</sup>	23.6 <sup>b</sup>	19.0 <sup>b</sup>	-0.6 <sup>b</sup>	-0.4 <sup>b,h</sup>	14.1 <sup>b</sup>	3.8 <sup>b</sup>	1.2 <sup>e</sup>									
3/Ru(II)	$\Delta\Delta G$	0.0 <sup>b,i</sup>	-5.3 <sup>b,i</sup>	-2.3 <sup>b,j</sup>	2.6 <sup>b,j</sup>	29.5 <sup>b,j</sup>	5.4 <sup>b,j</sup>	-5.2 <sup>b</sup>	14.8 <sup>b</sup>	24.5 <sup>e</sup>									
	$\Delta\Delta G^\ddagger$	0.0 <sup>b,i</sup>	-0.7 <sup>b,i</sup>	11.5 <sup>b,j</sup>	10.0 <sup>b,j</sup>	-6.7 <sup>b,j</sup>	-1.1 <sup>b,j</sup>	14.2 <sup>b</sup>	-0.3 <sup>b</sup>	-0.7 <sup>e</sup>									
4/Cu(II)	$\Delta\Delta G$	1.7 <sup>c,k</sup>	0.0 <sup>c,l</sup>	2.1 <sup>c,k</sup>	-0.7 <sup>c,k</sup>	19.3 <sup>c,k</sup>	2.7 <sup>c</sup>	1.2 <sup>d</sup>	7.4 <sup>d</sup>	8.3 <sup>c</sup>									
	$\Delta\Delta G^\ddagger$	0.1 <sup>c,k</sup>	0.0 <sup>c,l</sup>	13.5 <sup>c,k</sup>	15.8 <sup>c,k</sup>	-4.4 <sup>c,k</sup>	-1.1 <sup>c</sup>	11.8 <sup>d</sup>	-0.2 <sup>d</sup>	1.4 <sup>c</sup>									

<sup>a</sup>Compared with the reference reaction, positive  $\Delta\Delta G$  and  $\Delta\Delta G^\ddagger$  mean less favorable binding energy and higher barrier, respectively, and vice versa. <sup>b</sup> $\Delta G$  and  $\Delta G^\ddagger$  of **1b** as reference. <sup>c</sup> $\Delta G$  and  $\Delta G^\ddagger$  of **2a** as reference. <sup>d</sup> $\Delta G$  and  $\Delta G^\ddagger$  of **1a** as reference. <sup>e</sup> $\Delta G$  and  $\Delta G^\ddagger$  of **2b** as reference. <sup>f</sup>Reactive, see ref 8b. <sup>g</sup>Reactive, see ref 7c. <sup>h</sup>Reactive, this work. <sup>i</sup>Reactive, see ref 9c. <sup>j</sup>Not reactive, see ref 9c. <sup>k</sup>Not reactive, see ref 10b. <sup>l</sup>Reactive, see ref 10b.

accuracy limit of current approximate density functionals in computing the  $\Delta G$  and  $\Delta G^\ddagger$  values because the trend of energetics is more reliably followed in DFT calculation than the value of energetics.<sup>19</sup> All the computational results of  $\Delta\Delta G$  and  $\Delta\Delta G^\ddagger$  are summarized in Table 1, with the known experimental reactivity denoted to assist comparisons between the theory and experiments, and the  $\Delta G$  and  $\Delta G^\ddagger$  data are relegated to the SI (see Scheme S1).

### 3.1. The Pristine N,N-Bidentate Chelation Substrates.

First, let us explore the two types of pristine N,N-bidentate substrates **1** and **2**, which serve as the corresponding references to compare for other substrates. As shown in Scheme 3, the amide N coordination site in pristine substrates **1** and **2** enables cyclometalation to form a five-membered metallacycle upon C–H activation, which is a common structural feature for all those substrates with an amide directing group in Scheme 4. Experimentally, in the three reactions promoted by Ni, Pd, and Ru, both **2b** and **1b** are reactive,<sup>7c,8b,9c</sup> whereas in the Cu-mediated reaction, **2a** is reactive, but **1a** is not.<sup>10b</sup> In line with the experimental reactivity of Cu-mediated reactions with **2a** and **1a**,<sup>10b</sup> herein, we observed that the binding (Gibbs) free energy of **1a** is 1.7 kcal/mol less favorable than that of **2a** in Cu-promoted C–H activation reaction, whereas the barriers are only slightly different, by 0.1 kcal/mol, implying that it is the stronger substrate binding that makes **2a** more reactive toward C–H activation than **1a** in this reaction. More generally, the corresponding first two columns of data in Table 1 show that substrates **2b/2a** consistently coordinate to the metal more tightly than **1b/1a** by about 2–5 kcal/mol for all the reactions under study, albeit bearing very close C–H activation barriers. Interestingly, this computational result supports the recent conclusion of Chatani et al. that **2** has a bidentate directing group that is superior to that of **1**, for which a more acidic NH bond in 8-aminoquinoline than that in 2-pyridinylmethylamine was considered as an explanation.<sup>4</sup> Certainly, a more acidic NH bond would favor the substrate binding in energy due to easier NH deprotonation; thus, these two explanations are in mutual agreement.

### 3.2. The Effect of Proximal Coordinating Site.

As shown in Scheme 2, the substrate with a bidentate chelation directing group has two coordinating sites, one (P) is proximal to the C–H bond to be activated and the other (D) is at a distal position. Previously, changing the directing group PH from NH to O or NMe had been frequently explored experimentally.<sup>8b,9a,c,d,10b</sup> It was found that these substitutions in substrates never worked to render any reactivity. What is the reason for this phenomenon? One simple intuitive explanation would be that O and NMe bind to the metal center more weakly than the deprotonated NH; thus, substrates loose binding energy,  $\Delta G$ . Surprisingly, our computational results for **3**, **3-A**, **4**, and **4-A** in Table 1 reveal alternative origin for the inactivity of those substrates bearing O and NMe at the P positions.

First, we test the effect caused by NH-to-O substitution with substrates **3** and **3-A**, whose results are shown in the corresponding third column of data in Table 1. When **3** was employed as the substrate in the Ni(II)-catalyzed reaction, the C–H activation barrier was greatly increased by 26.1 kcal/mol compared with **1b**, although the substrate binding free energy is even more favored by 6.5 kcal/mol. This implies that the C–H activation barrier leads to the inaccessibility of **3** as the directing group for the Ni(II)-catalyzed reaction. Similarly, this C–H activation barrier-controlled reactivity with **3** or **3-A** is kept in the corresponding Pd(II), Ru(II), and Cu(II)-promoted C–H activation reactions. In these cases, substrate binding free energies are only slightly changed relative to the corresponding pristine substrates ( $\Delta\Delta G = -1.1$ ,  $-2.3$ , and  $2.1$  kcal/mol for Pd(II)-, Ru(II)-, and Cu(II)-promoted reactions, respectively). Obviously, the sizable C–H activation barrier increase ( $\Delta\Delta G^\ddagger = 23.6$ ,  $11.5$ , and  $13.5$  kcal/mol for Pd(II)-, Ru(II)-, and Cu(II)-promoted reactions, respectively) relative to its corresponding pristine substrates are too high to make **3** or **3-A** reactive, as in the Ni(II) case.

The origin for the inactivity of the substrate found above for **3** and **3-A** also holds true when using substrates **4** and **4-A** having NH-to-NMe substitution. As shown in the corresponding fourth column of data in Table 1, the rather large increases

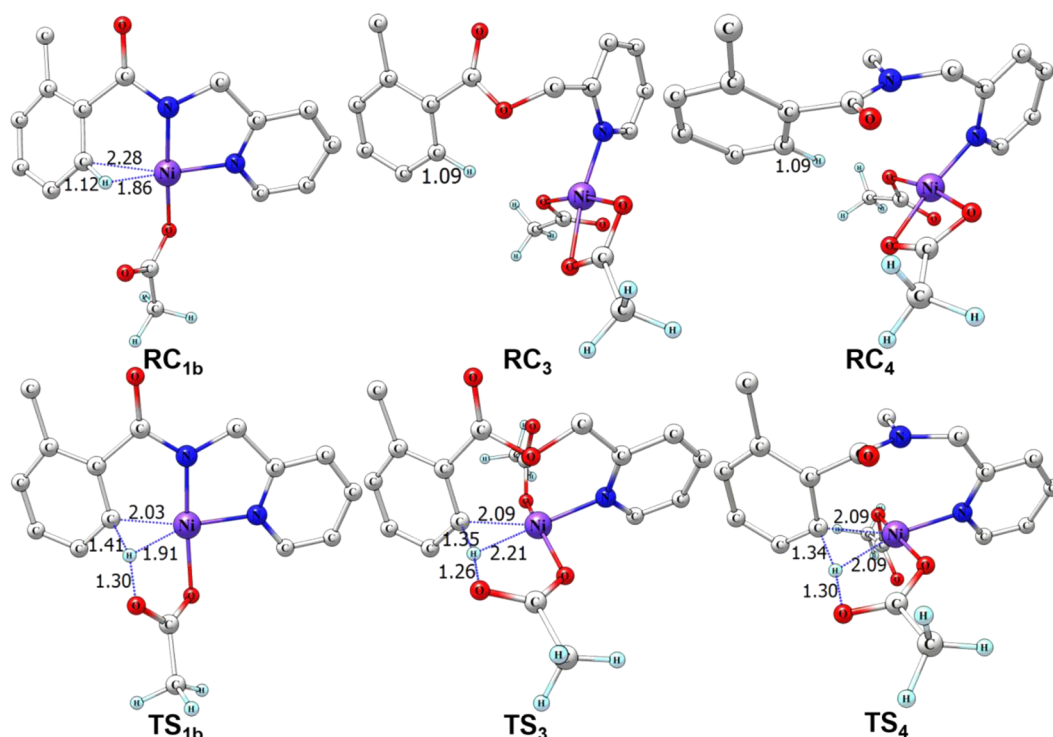


**Figure 1.** Optimized geometries of reactant complexes and transition states for P-substituted (by O and NMe) substrates ( $\text{RC}_3$ ,  $\text{RC}_4$ ,  $\text{TS}_3$ ,  $\text{TS}_4$ ) and the pristine substrate  $\text{1b}$  ( $\text{RC}_{1b}$ ,  $\text{TS}_{1b}$ ) involved in reaction 1. Hydrogen atoms on the substrates are omitted for clarity, except the transferred H. Unlike the pristine substrate  $\text{RC}_{1b}$ , two acetate ligands remain in the P-substituted systems to make them neutral.

in the C–H activation barrier ( $\Delta\Delta G^\ddagger = 22.8, 18.6, 10.0,$  and  $15.8$  kcal/mol for the Ni(II)-, Pd(II)-, Ru(II)-, and Cu(II)-promoted reactions, respectively) from changing the directing group NH to NMe, are dominant, and the changes in the substrate binding free energy are only minor ( $\Delta\Delta G = -5.6, -1.3, 2.6,$  and  $-0.7$  kcal/mol for the Ni(II)-, Pd(II)-, Ru(II)-, and Cu(II)-promoted reactions, respectively). Thus, it is the C–H activation barrier that controls these reactions with substrates **4** and **4-A**.

As elaborated above, our results demonstrate that changing proximal coordinating site P from NH to O and NMe will not necessarily disfavor the substrate binding, but will certainly cause a large increase in the C–H activation barrier, which makes these substrates inactive in the reaction. All the C–H activation barriers for **3**, **3-A**, **4**, and **4-A** are significantly higher than the corresponding pristine substrates, by at least 10 kcal/mol. This phenomenon of significant increase in the C–H activation barrier height could be associated with some structural feature of the reactant complex (RC). For example, as depicted in Figure 1 for Ni(II)-promoted reactions, although C–H activation TSs with substrates **1b**, **3**, and **4** ( $\text{TS}_{1b}$ ,  $\text{TS}_3$ , and  $\text{TS}_4$ ) are qualitatively similar in structure near the activated C–H moiety, their four-coordinate RCs ( $\text{RC}_{1b}$ ,  $\text{RC}_3$ , and  $\text{RC}_4$ ), which are linked directly by  $\text{TS}_{1b}$ ,  $\text{TS}_3$ , and  $\text{TS}_4$ , respectively, are quite different. The acetate ligand in  $\text{RC}_{1b}$  adopts a  $\kappa^1\text{-CO}_2^-$  coordination mode, whereas that in  $\text{RC}_3$  and  $\text{RC}_4$  takes a  $\kappa^2\text{-CO}_2^-$  coordination mode. As a result, to accept the transferred H from the breaking C–H bond,  $\text{TS}_3$  and  $\text{TS}_4$  would need to break one leg of  $\kappa^2\text{-CO}_2^-$  coordination to become  $\kappa^1\text{-CO}_2^-$  coordinated when evolving from the respective  $\text{RC}_3$  and  $\text{RC}_4$ , but from  $\text{RC}_{1b}$ ,  $\text{TS}_{1b}$  does not need to do so. This extra  $\kappa^2$ -to- $\kappa^1$  coordination transition makes the barrier of substrates **3** and **4** higher than that of the corresponding reference substrate **1b**. In

addition to the Ni(II)-promoted reaction, the analogous behavior is also observed for the P-substituted substrates (by O and NMe) in the Pd(II), Ru(II), and Cu(II)-promoted C–H bond activation reactions (for details, see the SI). In summary, our computational results clarify the pivotal role of the NH group in affecting the reactivity of the N,N-bidentate chelation directing groups, as considered by many recent experimental investigations.<sup>4,5,6e,7a,b,8b,9c,10b</sup>

**3.3. The Effect of Distal Coordinating Site.** Having clarified the consequence of introducing variations on the proximal P position, what will happen if the distal coordinate site D in Scheme 2 is changed? To explore this, we studied the substrates **5** and **5-A**, in which pyridinyl and quinolinyl groups are replaced by phenyl and naphthalenyl groups without strong coordinating ability. The corresponding results in Table 1 clearly indicate that this substitution will consistently cause the substrates to significantly lose the binding free energy, by  $\sim 20$ – $30$  kcal/mol, which is in good agreement with the available experimental results of the incapability of these and similar substrates in Ni-, Ru-, and Cu-promoted reactions.<sup>8b,9a,c,d,10b</sup> Specifically, for **5** in Ni(II), Pd(II), Ru(II), and Cu(II)-promoted C–H activation reactions, the substrate binding free energies,  $\Delta G$ , are disfavored by 25.9, 20.1, 29.5, and 19.3 kcal/mol compared with the corresponding pristine substrates; however, the C–H activation barriers are all correspondingly lowered by 0.9, 0.6, 6.7, and 4.4 kcal/mol for the above four reactions. These results indicate that the distal site D affects more the substrate binding free energy. Consequently, in contrast to P site variations, all barriers arising from the D site replacement are lowered to some extent, which demonstrates that the D site coordination weakening will not necessarily result in increasing C–H activation barriers.

**Table 2.** Key Bond Lengths (in Å) of the Reactant Complex (RC) and Transition State (TS) for One-Carbon-Shorter Substrate 7 and Pristine Substrate 1 Involved in Reactions 1–4

substrate:	$R_{M-N(Py)}/R_{M-N(amide)}$							
	1b			1a	7b			7a
metal:	Ni	Pd	Ru	Cu	Ni	Pd	Ru	Cu
RC	1.90/1.84	2.04/1.97	2.06/2.04	1.99/1.94	1.89/1.93	2.02/2.05	2.05/2.21	1.93/2.02
TS	1.93/1.83	2.08/1.95	2.13/2.03	2.06/1.90	2.02/1.82	2.24/1.94	2.23/2.01	2.07/1.93
$\Delta R_{TS-RC}$	0.03/−0.01	0.04/−0.02	0.07/−0.01	0.07/−0.04	0.13/−0.11	0.22/−0.11	0.18/−0.20	0.14/−0.09

**3.4. The Effects of Enlarging and Shrinking Chelation Ring.** After binding to the metal center, the N,N-bidentate directing group in the pristine substrate **1** or **2** forms a five-membered ring with the metal through chelation. What effect will be brought if this ring is expanded to a six-membered ring or shrunk to a four-membered ring? To answer this question, we studied substrates **6**, **6-A**, and **7**, which have longer or shorter alkyl chain compared with **1** and **2**.

For six-membered ring chelation, our results on **6** and **6-A** as shown in Table 1 indicate that the resultant effect is metal-dependent. For the Ni(II)-catalyzed C–H bond activation reaction, the binding free energy of **6** is disfavored by 3.3 kcal/mol compared with the pristine substrate **1b**, and the C–H activation barrier also increases by 1.8 kcal/mol, indicating that both the substrate binding free energy and the C–H activation barrier contribute to the decreased reactivity of **6**. Recent experimental investigation showed that **6** was not reactive in Ru-promoted reactions.<sup>9c</sup> According to our results, this could be explained only by the binding free energy loss, not by the barrier change, because substrate binding free energy of **6** is disfavored by 5.4 kcal/mol relative to the pristine substrate **1b**, whereas the C–H activation barrier is lowered by 1.1 kcal/mol. Similar decreased reactivity controlled by the substrate binding free energy, such as in the Ru-promoted reaction, was found in the Cu(II)-promoted C–H bond activation reaction with substrate **6-A**, as well, as reflected by the 2.7 kcal/mol disfavoring of substrate binding free energy, but 1.1 kcal/mol favoring in the C–H activation barrier relative to the reference substrate **2a**. For Pd with substrate **6**, however, our calculation indicates that its binding energy increases only slightly, by 0.5 kcal/mol, and its barrier decreases slightly, by 0.4 kcal/mol, compared with those of **1b**. Thus, in total, the effective barrier of reaction is almost unaffected. Hence, we predict that substrate **6** in a reaction promoted by Pd<sup>7c</sup> should be reactive.

To test this computational prediction, we conducted the corresponding experiment. In good agreement with theory, we found that **6** was reactive in a reaction promoted by Pd<sup>7c</sup> and we got similar yields for pristine substrate **1b** (55%) and **6** (47%). This result shows that our reaction model and comparative analysis approach are reasonable to give a correct prediction on the reactivity.

Interestingly, concerning the one-carbon-shorter substrate **7** that can form only a four-membered ring through chelation with a metal, a trend different from the one-carbon-longer substrates (**6** and **6-A**) is discovered. From the seventh column of data in Table 1, it is apparent that the C–H activation barriers for substrates **7** are significantly increased, by 16.5, 14.1, 14.2, and 11.8 kcal/mol, in Ni(II)-, Pd(II)-, Ru(II)-, and Cu(II)-promoted C–H bond activation reactions when compared with their respective reference substrates **1**. Meanwhile, the substrate binding free energies of **7** are much less affected and also not in a uniform direction, as indicated by their energy shifts of −4.5, −1.6, −5.2, and 1.2 kcal/mol away

from the corresponding values of substrates **1**. Thus, the barrier increasing factor will dominate the C–H activation process for a one-carbon-shorter substrate. This result can be explained by the structural deformation in the C–H bond breakage process. In Table 2, we compare the bond lengths of two metal–nitrogen bonds in bidentate chelation for TSs and RCs of all reactions with **1** and **7** as substrates. When **7** are the substrates, the bond length variation from RC to TS (0.09–0.22 Å) is much larger than that of **1** (0.01–0.07 Å), which clearly indicates that a larger structural deformation of the bidentate group has to be encountered in the case of a four-membered ring. This will certainly cost more energy with a C–H activation barrier. Experimentally, substrates bearing a N,N-bidentate directing group with a one-carbon-shorter alkyl chain, such as **7**, were never found reactive in Ni- and Ru-promoted reactions,<sup>6o,p,8a,9a,b</sup> which is in line with our computational results of significant barrier height increase.

Combined with the results for longer alkyl chain substrates **6** and **6-A**, we here conclude that changing the N,N-bidentate chelating ring size can change the reactivity by affecting either the substrate binding or the C–H activation barrier, depending on the metal identity and ring size.

**3.5. The Effect of Chelation.** Finally, to explore the effect of chelation itself by N,N-bidentate directing groups, we studied **8** and **9** with no chelation at all. As shown in the second-last column of data in Table 1, compared with the corresponding reference substrates **1** (**1b** and **1a**), the substrate binding free energies of **8** (**8b** and **8a**) are disfavored by 9.3, 7.5, 14.8, and 7.4 kcal/mol for all reactions promoted by Ni, Pd, Ru, and Cu, respectively, but the C–H activation barrier was affected less significantly, by 6.1, 3.8, −0.3, −0.2 kcal/mol, respectively. Hence, these results in Table 1 indicate that the main effect exerted by chelation is to enhance the substrate binding strength of substrates **8** by about 7–14 kcal/mol. The barrier changes are more limited in magnitude and not uniform in direction.

The substrate binding-controlled reactivity found in **8** also manifests itself well in **9**, as observed in the last column of data in Table 1. One notable quantitative difference between **8** and **9** is the degree of enhancement in the substrate binding free energy,  $\Delta\Delta G$ . The substrate coordination strength enhancement gained through chelation from **9** to its pristine **2** is generally larger than that from **8** to its pristine **1**. This is in accord with the fact that the quinolinyl directing group in **2** has a more rigid backbone than the pyridinyl one in **1**. The rigidity of the former directing group will help to generate a tighter substrate binding by decreasing the entropic contribution in free energy.

To gain more insight into the origin of losing the substrate binding free energy for substrates without bidentate chelation, we analyzed the two components of  $\Delta\Delta G$  for **8** and **9**. One component is the electronic energy component,  $\Delta\Delta E$ , that also includes the DFT-D3 dispersion contribution; the other

**Table 3.** The Calculated Components ( $\Delta\Delta G_{\text{Gibbs}}$  and  $\Delta\Delta E$ ) of Relative Free Energy ( $\Delta\Delta G$ ) for Substrates **8** and **9** (in kcal/mol) without Bidentate Chelation<sup>a</sup>

	substrate/metal							
	8b/Ni <sup>b</sup>	8b/Pd <sup>b</sup>	8b/Ru <sup>b</sup>	8a/Cu <sup>c</sup>	9b/Ni <sup>d</sup>	9b/Pd <sup>d</sup>	9b/Ru <sup>d</sup>	9a/Cu <sup>c</sup>
$\Delta\Delta G_{\text{Gibbs}}$	14.2	13.5	16.0	14.0	15.3	14.5	17.7	16.1
$\Delta\Delta E$	-4.9	-6.0	-1.2	-6.6	-1.1	-1.0	6.8	-7.8
$\Delta\Delta G$	9.3	7.5	14.8	7.4	14.2	13.5	24.5	8.3

<sup>a</sup> $\Delta\Delta G = \Delta\Delta G_{\text{Gibbs}} + \Delta\Delta E$ .  $\Delta\Delta G_{\text{Gibbs}}$  is the gas phase thermal free energy correction component of Gibbs free energy;  $\Delta\Delta E$  is the electronic energy (in solution, including DFT-D3 dispersion correction) component of the Gibbs free energy. <sup>b</sup>Taking **1b** as reference. <sup>c</sup>Taking **1a** as reference. <sup>d</sup>Taking **2b** as reference. <sup>e</sup>Taking **2a** as reference.

component is the thermal Gibbs free energy correction,  $\Delta\Delta G_{\text{Gibbs}}$ , that includes the entropic contribution. The results shown in Table 3 demonstrate clearly that  $\Delta\Delta G_{\text{Gibbs}}$  is the dominant component of  $\Delta\Delta G$ . For example, in the Ru(II)-catalyzed C–H bond activation reaction (reaction 3), the  $\Delta\Delta G_{\text{Gibbs}}$  in **8b** contributes 16.0 kcal/mol to  $\Delta\Delta G$  (14.8 kcal/mol), as compared with the -1.2 kcal/mol contribution from  $\Delta\Delta E$ .

#### 4. CONCLUSIONS

In summary, in this work, we have systematically studied and analyzed the factors that affect the reactivity of transition-metal-promoted C(sp<sup>2</sup>)-H activation assisted by N,N-bidentate directing groups. The reactions under study cover the most representative transition metals employed in C(sp<sup>2</sup>)-H activation by N,N-double coordination strategy, including Ni, Pd, Ru, and Cu, and a plethora of substrates are investigated. Through a theoretical approach characterized by comparison between different substrates, we found that (1) quinolinyl directing groups are generally more reactive than pyridinyl ones because the former bind metal more tightly. (2) In the two coordination sites of the N,N-bidentate directing group, the one proximal to the C–H bond to be activated influences the C–H activation barrier more, whereas the distal site affects the substrate binding energy more. (3) Enlarging/shrinking the chelation ring of N,N-bidentate directing groups can exert different effects on the reactivity, depending on the metal identity and the ring size. (4) Bidentate chelation generally leads to a tighter substrate binding. These findings and rationales for reactivity are consistent with all the relevant experimental results to date. In addition, our theoretical prediction for reactivity of a substrate is confirmed by the experiment conducted in this work, which lends more credence to the theory. The rationale behind the N,N-bidentate directing group strategy revealed in our work would help one to better understand and improve this promising C–H activation approach. Further extensions of the reactivity theory obtained in this work to other types of bidentate directing groups as well as to inert C(sp<sup>3</sup>)-H activation are appealing. These studies utilizing the informative theoretical approach of comparative analysis presented in this work are currently underway in our laboratories.

#### ■ ASSOCIATED CONTENT

##### Supporting Information

Experimental procedures, Cartesian coordinates, computational results, and spectroscopic data. This information is available free of charge via the Internet at <http://pubs.acs.org>.

#### ■ AUTHOR INFORMATION

##### Corresponding Authors

\*E-mail: [huangxr@jlu.edu.cn](mailto:huangxr@jlu.edu.cn) (X.H.).

\*E-mail: [wangcy@iccas.ac.cn](mailto:wangcy@iccas.ac.cn) (C.W.).

\*E-mail: [chenh@iccas.ac.cn](mailto:chenh@iccas.ac.cn) (H.C.).

##### Notes

The authors declare no competing financial interest.

#### ■ ACKNOWLEDGMENTS

Generous financial supports from the National Natural Science Foundation of China (21290194, 21002103, 21221002), the National Basic Research Program of China (973 Program) (No. 2012CB821600), and Institute of Chemistry, CAS, are gratefully acknowledged.

#### ■ REFERENCES

- (1) For some recent reviews of C–H bond functionalization, see: (a) Lersch, M.; Tilset, M. *Chem. Rev.* **2005**, *105*, 2471–2526. (b) Kakiuchi, F.; Kochi, T. *Synthesis* **2008**, 3013–3039. (c) McGlacken, G. P.; Bateman, L. M. *Chem. Soc. Rev.* **2009**, *38*, 2447–2464. (d) Daugulis, O.; Do, H.-Q.; Shabashov, D. *Acc. Chem. Res.* **2009**, *42*, 1074–1086. (e) Chen, X.; Engle, K. M.; Wang, D.-H.; Yu, J.-Q. *Angew. Chem., Int. Ed.* **2009**, *48*, 5094–5115. (f) Ackermann, L.; Vicente, R.; Kapdi, A. R. *Angew. Chem., Int. Ed.* **2009**, *48*, 9792–9826. (g) Colby, D. A.; Bergman, R. G.; Ellman, J. A. *Chem. Rev.* **2010**, *110*, 624–655. (h) Sehnaal, P.; Taylor, R. J. K.; Fairlamb, I. J. S. *Chem. Rev.* **2010**, *110*, 824–889. (i) Wendlandt, A. E.; Suess, A. M.; Stahl, S. S. *Angew. Chem., Int. Ed.* **2011**, *50*, 11062–11087. (j) Ackermann, L. *Chem. Commun.* **2010**, *46*, 4866–4877. (k) Mkhallid, I. A. I.; Barnard, J. H.; Marder, T. B.; Murphy, J. M.; Hartwig, J. F. *Chem. Rev.* **2010**, *110*, 890–931. (l) Sun, C.-L.; Li, B.-J.; Shi, Z.-J. *Chem. Rev.* **2011**, *111*, 1293–1314. (m) Chen, D. Y.-K.; Youn, S. W. *Chem.—Eur. J.* **2012**, *18*, 9452–9474. (n) Yamaguchi, J.; Yamaguchi, A. D.; Itami, K. *Angew. Chem., Int. Ed.* **2012**, *51*, 8960–9009. (o) Li, B.-J.; Shi, Z.-J. *Chem. Soc. Rev.* **2012**, *41*, 5588–5598. (p) Newhouse, T.; Baran, P. S. *Angew. Chem., Int. Ed.* **2011**, *51*, 3362–3374. (q) Kuhl, N.; Hopkinson, M. N.; Wencel-Delord, J.; Glorius, F. *Angew. Chem., Int. Ed.* **2012**, *51*, 10236–10254. (r) Boorman, T. C.; Larrosa, I. *Chem. Soc. Rev.* **2011**, *40*, 1910–1925. (s) Collet, F.; Lescot, C.; Dauban, P. *Chem. Soc. Rev.* **2011**, *40*, 1926–1936. (t) Cho, S. H.; Kim, J. Y.; Kwak, J.; Chang, S. *Chem. Soc. Rev.* **2011**, *40*, 5068–5083. (u) Che, C.-M.; Lo, V. K.-Y.; Zhou, C.-Y.; Huang, J.-S. *Chem. Soc. Rev.* **2011**, *40*, 1950–1975. (v) Mousseau, J.; Charette, A. B. *Acc. Chem. Res.* **2013**, *46*, 412–424. (w) Kozhushkov, S. I.; Ackermann, L. *Chem. Sci.* **2013**, *4*, 886–896.
- (2) (a) Murai, S.; Kakiuchi, F.; Sekine, S.; Tanaka, Y.; Kamatani, A.; Sonoda, M.; Chatani, N. *Nature* **1993**, *366*, 529–531. (b) Ritleng, V.; Sirlin, C.; Pfeffer, M. *Chem. Rev.* **2002**, *102*, 1731–1769. (c) Daugulis, O.; Zaitsev, V. G.; Shabashov, D.; Pham, Q. N.; Lazareva, A. *Synlett* **2006**, 3382–3388. (d) Alberico, D.; Scott, M. E.; Lautens, M. *Chem. Rev.* **2007**, *107*, 174–238. (e) Chen, X.; Engle, K. M.; Wang, D. H.; Yu, J.-Q. *Angew. Chem., Int. Ed.* **2009**, *48*, 5094–5115. (f) Lyons, T. W.; Sanford, M. S. *Chem. Rev.* **2010**, *110*, 1147–1169. (g) Ackermann, L. *Chem. Rev.* **2011**, *111*, 1315–1345. (h) Yeung, C. S.; Dong, V. M. *Chem. Rev.* **2011**, *111*, 1215–1292. (i) Neufeldt, S. R.; Sanford, M. S.

- Acc. Chem. Res.* **2012**, *45*, 936–946. (j) Engle, K. M.; Mei, T. S.; Wasa, M.; Yu, J.-Q. *Acc. Chem. Res.* **2012**, *45*, 788–802. (k) Colby, D. A.; Tsai, A. S.; Bergman, R. G.; Ellman, J. *Acc. Chem. Res.* **2012**, *45*, 814–825. (l) Arockiam, P. B.; Bruneau, C.; Dixneuf, P. H. *Chem. Rev.* **2012**, *112*, 5879–5918. (m) Wang, C. *Synlett* **2013**, *24*, 1606–1613.
- (3) For a recent general review on computational studies, see: Balcells, D.; Clot, E.; Eisenstein, O. *Chem. Rev.* **2010**, *110*, 749–823 and references therein.
- (4) Rouquet, G.; Chatani, N. *Angew. Chem., Int. Ed.* **2013**, *52*, 11726–11743.
- (5) Zaitsev, V.; Shabashov, D.; Daugulis, O. *J. Am. Chem. Soc.* **2005**, *127*, 13154–13155. For a recent review, see: Corbet, M.; De Campo, F. *Angew. Chem., Int. Ed.* **2013**, *52*, 9896–9898.
- (6) C(sp<sup>3</sup>)-H activation, Pd: (a) Reddy, B. V. S.; Reddy, L. R.; Corey, E. J. *Org. Lett.* **2006**, *8*, 3391–3394. (b) Giri, R.; Mangel, N.; Foxman, B. M.; Yu, J.-Q. *Organometallics* **2008**, *27*, 1667–1670. (c) Feng, Y.; Chen, G. *Angew. Chem., Int. Ed.* **2010**, *49*, 958–961. (d) Feng, Y.; Wang, Y.; Landgraf, B.; Liu, S.; Chen, G. *Org. Lett.* **2010**, *12*, 3414–3417. (e) Ano, Y.; Tobisu, M.; Chatani, N. *J. Am. Chem. Soc.* **2011**, *133*, 12984–12986. (f) He, G.; Chen, G. *Angew. Chem., Int. Ed.* **2011**, *50*, 5192–5196. (g) Xie, Y.; Yang, Y.; Huang, L.; Zhang, X.; Zhang, Y. *Org. Lett.* **2012**, *14*, 1238–1241. (h) Tran, L. D.; Daugulis, O. *Angew. Chem., Int. Ed.* **2012**, *51*, 5188–5191. (i) Gutekunst, W. R.; Gianatassio, R.; Baran, P. S. *Angew. Chem., Int. Ed.* **2012**, *51*, 7507–7510. (j) Rit, R. K.; Yadav, M. R.; Sahoo, A. K. *Org. Lett.* **2012**, *14*, 3724–3727. (k) Zhang, S.-Y.; He, G.; Nack, W. A.; Zhao, Y.; Li, Q.; Chen, G. *J. Am. Chem. Soc.* **2013**, *135*, 2124–2127. (l) Zhang, S.-Y.; Li, Q.; He, G.; Nack, W. A.; Chen, G. *J. Am. Chem. Soc.* **2013**, *135*, 12135–12141. (m) Chen, K.; Hu, F.; Zhang, S.-Q.; Shi, B.-F. *Chem. Sci.* **2013**, *4*, 3906–3911. (n) He, G.; Zhang, S.-Y.; Nack, W. A.; Li, Q.; Chen, G. *Angew. Chem., Int. Ed.* **2013**, *52*, 11124–11128. (o) Parella, R.; Gopalakrishnan, B.; Babu, S. A. *J. Org. Chem.* **2013**, *78*, 11911–11934. (p) Parella, R.; Gopalakrishnan, B.; Babu, S. A. *Org. Lett.* **2013**, *15*, 3238–3241. (q) Roman, D. S.; Charette, A. B. *Org. Lett.* **2013**, *15*, 4394–4397. For a few available examples of C(sp<sup>3</sup>)-H activation by other transition metals, Fe: (r) Shang, R.; Ilies, L.; Matsumoto, A.; Nakamura, E. *J. Am. Chem. Soc.* **2013**, *135*, 6030–6032. (s) Asako, S.; Ilies, L.; Nakamura, E. *J. Am. Chem. Soc.* **2013**, *135*, 17755–17757. (t) Matsubara, T.; Asako, S.; Ilies, L.; Nakamura, E. *J. Am. Chem. Soc.* **2014**, *136*, 646–649. Ru: (u) Hasegawa, N.; Charra, V.; Inoue, S.; Fukumoto, Y.; Chatani, N. *J. Am. Chem. Soc.* **2011**, *133*, 8070–8073. (v) Hasegawa, N.; Shibata, K.; Charra, V.; Inoue, S.; Fukumoto, Y.; Chatani, N. *Tetrahedron* **2013**, *69*, 4466–4472. Ni: (w) Aihara, Y.; Chatani, N. *J. Am. Chem. Soc.* **2014**, *136*, 898–901.
- (7) C(sp<sup>2</sup>)-H activation, Pd: (a) Gou, F.-R.; Wang, X.-C.; Huo, P.-F.; Bi, H.-P.; Guan, Z.-H.; Liang, Y.-M. *Org. Lett.* **2009**, *11*, 5726–5729. (b) Shabashov, D.; Daugulis, O. *J. Am. Chem. Soc.* **2010**, *132*, 3965–3972. (c) Ano, Y.; Tobisu, M.; Chatani, N. *Org. Lett.* **2012**, *14*, 354–357. (d) Zhao, Y.; Chen, G. *Org. Lett.* **2011**, *13*, 4850–4853. (e) He, G.; Lu, C.; Zhao, Y.; Nack, W. A.; Chen, G. *Org. Lett.* **2012**, *14*, 2944–2947. (f) Zhao, Y.; He, G.; Nack, W. A.; Chen, G. *Org. Lett.* **2012**, *14*, 2948–2951. (g) He, G.; Zhao, Y.; Zhang, S.; Lu, C.; Chen, G. *J. Am. Chem. Soc.* **2012**, *134*, 3–6. (h) Nadres, E. T.; Daugulis, O. *J. Am. Chem. Soc.* **2012**, *134*, 7–10. (i) Zhang, S.-Y.; He, G.; Zhao, Y.; Wright, K.; Nack, W. A.; Chen, G. *J. Am. Chem. Soc.* **2012**, *134*, 7313–7316. (j) Chen, F.-J.; Zhao, S.; Hu, F.; Chen, K.; Zhang, Q.; Zhang, S.-Q.; Shi, B.-F. *Chem. Sci.* **2013**, *4*, 4187–4192. (k) Ye, X. H.; He, Z. R.; Ahmed, T.; Weise, K.; Akhmedov, N. G.; Petersen, J. L.; Shi, X. D. *Chem. Sci.* **2013**, *4*, 3712–3716. (l) Nadres, E. T.; Santos, G. I. F.; Shabashov, D.; Daugulis, O. *J. Org. Chem.* **2013**, *78*, 9689–9714. (m) Mei, T. S.; Leow, D.; Xiao, H.; Laforteza, B. N.; Yu, J.-Q. *Org. Lett.* **2013**, *15*, 3058–3061. (n) Nack, W. A.; He, G.; Zhang, S.-Y.; Lu, C. X.; Chen, G. *Org. Lett.* **2013**, *15*, 3440–3443.
- (8) C(sp<sup>2</sup>)-H activation, Ni: (a) Shiota, H.; Ano, Y.; Aihara, Y.; Fukumoto, Y.; Chatani, N. *J. Am. Chem. Soc.* **2011**, *133*, 14952–14955. (b) Aihara, Y.; Chatani, N. *J. Am. Chem. Soc.* **2013**, *135*, 5308–5311.
- (9) C(sp<sup>2</sup>)-H activation, Ru: (a) Inoue, S.; Shiota, H.; Fukumoto, Y.; Chatani, N. *J. Am. Chem. Soc.* **2009**, *131*, 6898–6899. (b) Shibata, K.; Hasegawa, N.; Fukumoto, Y.; Chatani, N. *ChemCatChem* **2012**, *4*, 1733–1736. (c) Aihara, Y.; Chatani, N. *Chem. Sci.* **2013**, *4*, 664–670. (d) Rouquet, G.; Chatani, N. *Chem. Sci.* **2013**, *4*, 2201–2208.
- (10) C(sp<sup>2</sup>)-H activation, Cu: (a) Tran, L. D.; Popov, I.; Daugulis, O. *J. Am. Chem. Soc.* **2012**, *134*, 18237–18240. (b) Nishino, M.; Hirano, K.; Satoh, T.; Miura, M. *Angew. Chem., Int. Ed.* **2013**, *52*, 4457–4461. (c) Tran, L. D.; Roane, J.; Daugulis, O. *Angew. Chem., Int. Ed.* **2013**, *52*, 6043–6046. (d) Truong, T.; Klimovica, K.; Daugulis, O. *J. Am. Chem. Soc.* **2013**, *135*, 9342–9345. (e) Odani, R.; Hirano, K.; Satoh, T.; Miura, M. *J. Org. Chem.* **2013**, *78*, 11045–11052. (f) Roane, J.; Daugulis, O. *Org. Lett.* **2013**, *15*, 5842–5845. (g) Suess, A. M.; Ertem, M.; Cramer, C. J.; Stahl, S. S. *J. Am. Chem. Soc.* **2013**, *135*, 9797–9804.
- (11) Some selected theoretical studies on monodentate directing groups: (a) Matsubara, T.; Koga, N.; Musaev, D. G.; Morokuma, K. *J. Am. Chem. Soc.* **1998**, *120*, 12692–12693. (b) Davies, D. L.; Donald, S. M. A.; Macgregor, S. A. *J. Am. Chem. Soc.* **2005**, *127*, 13754–13755. (c) Zhou, B.; Chen, H.; Wang, C. *J. Am. Chem. Soc.* **2013**, *135*, 1264–1267. (d) Clot, E.; Chen, J.; Lee, D.-H.; Sung, S. Y.; Appelhans, L. N.; Faller, J. W.; Crabtree, R. H.; Eisenstein, O. *J. Am. Chem. Soc.* **2004**, *126*, 8795–8804.
- (12) (a) Cross, W. B.; Hope, E. G.; Lin, Y.-H.; Macgregor, S. A.; Singh, K.; Solan, G. A.; Yahya, N. *Chem. Commun.* **2013**, *49*, 1918–1920. (b) Huang, L.; Li, Q.; Wang, C.; Qi, C. *J. Org. Chem.* **2013**, *78*, 3030–3038.
- (13) Frisch, M. J.; Trucks, G. W.; Schlegel, H. B.; Scuseria, G. E.; Robb, M. A.; Cheeseman, J. R.; Scalmani, G.; Barone, V.; Mennucci, B.; Petersson, G. A.; Nakatsuji, H.; Caricato, M.; Li, X.; Hratchian, H. P.; Izmaylov, A. F.; Bloino, J.; Zheng, G.; Sonnenberg, J. L.; Hada, M.; Ehara, M.; Toyota, K.; Fukuda, R.; Hasegawa, J.; Ishida, M.; Nakajima, T.; Honda, Y.; Kitao, O.; Nakai, H.; Vreven, T.; Montgomery, J. A., Jr.; Peralta, J. E.; Ogliaro, F.; Bearpark, M.; Heyd, J. J.; Brothers, E.; Kudin, K. N.; Staroverov, V. N.; Kobayashi, R.; Normand, J.; Raghavachari, K.; Rendell, A.; Burant, J. C.; Iyengar, S. S.; Tomasi, J.; Cossi, M.; Rega, N.; Millam, J. M.; Klene, M.; Knox, J. E.; Cross, J. B.; Bakken, V.; Adamo, C.; Jaramillo, J.; Gomperts, R.; Stratmann, R. E.; Yazyev, O.; Austin, A. J.; Cammi, R.; Pomelli, C.; Ochterski, J. W.; Martin, R. L.; Morokuma, K.; Zakrzewski, V. G.; Voth, G. A.; Salvador, P.; Dannenberg, J. J.; Dapprich, S.; Daniels, A. D.; Farkas, O.; Foresman, J. B.; Ortiz, J. V.; Cioslowski, J.; Fox, D. J. *Gaussian 09, revision C.01*; Gaussian, Inc.: Wallingford CT, 2010.
- (14) (a) Becke, A. D. *Phys. Rev. A* **1988**, *38*, 3098–3100. (b) Lee, C.; Yang, W.; Parr, R. G. *Phys. Rev. B* **1988**, *37*, 785–789. (c) Becke, A. D. *J. Chem. Phys.* **1993**, *98*, 5648–5652. (d) Becke, A. D. *J. Chem. Phys.* **1993**, *98*, 1372–1377. (e) Stephens, P. J.; Devlin, F. J.; Frisch, M. J.; Chabalowski, C. F. *J. Phys. Chem.* **1994**, *98*, 11623–11627.
- (15) Weigend, F.; Ahlrichs, R. *Phys. Chem. Chem. Phys.* **2005**, *7*, 3297–3305.
- (16) Marenich, A. V.; Cramer, C. J.; Truhlar, D. G. *J. Phys. Chem. B* **2009**, *113*, 6378–6396.
- (17) Grimme, S.; Antony, J.; Ehrlich, S.; Krieg, H. *J. Chem. Phys.* **2010**, *132*, 154104.
- (18) Fersht, A. *Structure and Mechanism in Protein Science: A Guide to Enzyme Catalysis and Protein Folding*; Freeman: New York, 1999.
- (19) (a) Lai, W. Z.; Yao, J. N.; Shaik, S.; Chen, H. *J. Chem. Theory Comput.* **2012**, *8*, 2991–2996. (b) Kang, R. H.; Lai, W. Z.; Yao, J. N.; Shaik, S.; Chen, H. *J. Chem. Theory Comput.* **2012**, *8*, 3119–3127. (c) Kang, R. H.; Yao, J. N.; Chen, H. *J. Chem. Theory Comput.* **2013**, *8*, 1872–1879. (d) Sun, Y. Y.; Chen, H. *J. Chem. Theory Comput.* **2013**, *9*, 4735–4743.